1.3 What is the resolution?

The resolution of the microscope determines the smallest feature that can just be resolved, or the smallest distance that can be determined between features. Although vital for microscopy, resolution is not easily defined in general terms. The attainable resolution depends strongly on the signal-to-noise ratio (SNR) of the imaging system, on the imaging mode, and (sometimes strongly) on *a priori* knowledge of the specimen. An often-used resolution criterion is the Rayleigh criterion, which was first developed in connection with the resolving power of prism and grating spectroscopes. It states that two components of equal intensity should be considered to be just resolved when the principal intensity maximum of one coincides with the first intensity minimum of the other [Born and Wolf, 1980] (see Fig. 1.12). For this situation, an approximately 20% drop in intensity occurs between the two maxima (depending on the shape of the distributions).

But what is the effect of noise? In other words, what is the relation between the SNR of the measurement and the attainable resolution? The SNR is defined as

$$\mathrm{SNR} = \frac{|\text{mean signal} - \text{background}|}{\text{signal standard deviation}}. \tag{1.13}$$

All kinds of noise, e.g., shot, thermal, read-out, photon statistical, photon-scattering, and quantization, affect either the background level or the signal's standard deviation and will therefore decrease the SNR of the system. A decrease in SNR in turn decreases the visibility of the intensity decrease between the maxima as specified by the Rayleigh criterion. As an illustration, consider a fundamental property of any measurement of photons: Poisson noise. It can be shown [Goodman, 1985] that the measurement of a large number of uncorrelated and discrete events, such as the arrival of photons at a photodetector, will give rise to so-called Poisson statistics.

For instance, consider the detection of fluorescence emitted from a sample. The sample emits photons at a certain average rate, but the individual photons are ran-

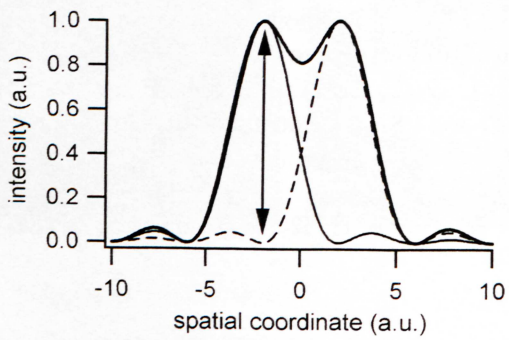

Figure 1.12 The Rayleigh criterion. Two components of equal intensity are resolved when the maximum of one coincides with the first minimum of the other. This results in an effective drop of the intensity between the two maxima of ~20%.

domly distributed over time. To determine the average fluorescence rate, the total number of photons emitted over a given time interval can be measured. Because of the random arrival of photons at the detector, repeating the measurement will yield a distribution of values. Hence, there remains an uncertainty in the true average value. For Poisson processes in particular, it means that if N photons are measured in a particular measurement, there is a 63% probability that the true average value is in the range between $N + \sqrt{N}$ and $N - \sqrt{N}$. For example, if N is 100 detected photons, a 63% probability exists that the true average value is in the range from 90 to 110. Because Poisson noise scales with $\sqrt{N}$, increasing the precision 10-fold, from $\pm 10\%$ to $\pm 1\%$, requires increasing the number of detected photons by a factor of 100, from 100 to 10,000. Poisson noise is an intrinsic property related to the detection of uncorrelated and discrete quantum events and cannot be avoided. Its relative importance can only be reduced by detecting as many photons as possible.

It is thus clear that whether the Rayleigh criterion is appropriate or not depends critically on the number of photons detected. To illustrate this point, consider the results of a numerical simulation shown in Fig. 1.13. The simulation involves the

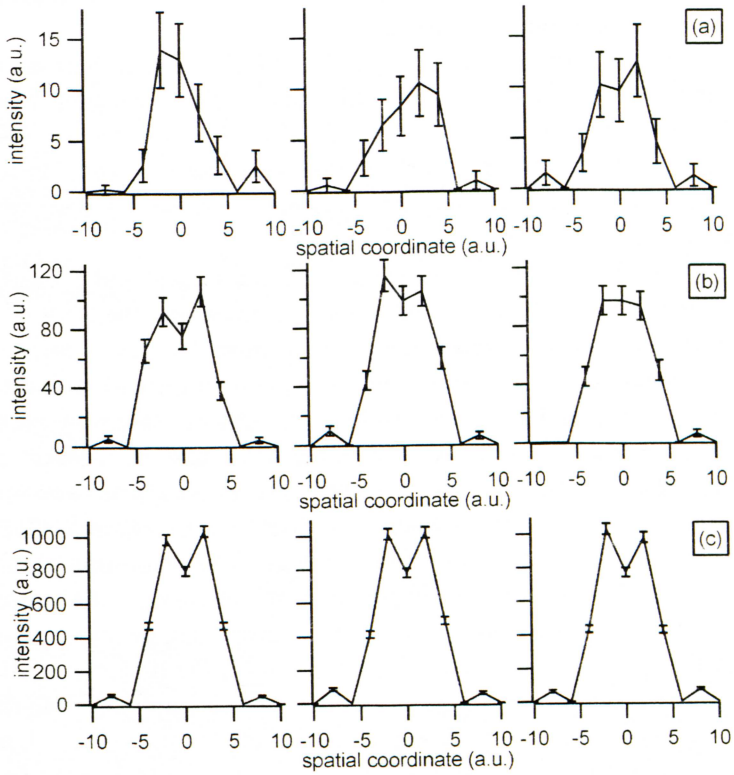

Figure 1.13 The influence of Poisson noise between two distributions, shifted spatially such that the maximum of the one coincides with the first minimum of the other (Rayleigh criterion). In this example, on average (a) 10, (b) 100, and (c) 1000 photons are detected from each intensity maximum. The reproducibility of each measurement is illustrated by the three subsequent measurements shown horizontally for each case.

measurement of photons emitted by two equally bright point sources that are separated by a distance exactly equal to the Rayleigh criterion. The signal is sampled along the spatial coordinate with a frequency that equals the Nyquist criterion. According to this criterion, a signal is sampled without artifacts only when it is sampled at a minimum of twice the frequency of the highest frequency present in the signal (see Chapter 4). In the case of the two point sources considered here, that corresponds to a sampling frequency of two samples per full-width-at-half-maximum (FWHM) of the signal distribution as a result of a single point source.

The difference between the simulated measurements shown in Figs. 1.13(a–c) is the maximum number of photons that are detected in each case. In Fig. 1.13(a) the maximum signal is on average 10 photons, whereas in Figs. 1.13(b) and 1.13(c) this number is 100 and 1000 photons respectively. It is assumed that only Poisson noise influences the measurement. Horizontally, three subsequent measurements are shown, where the changes are because of the random noise. The error bars denote the uncertainty in each measured value. The relative error of the measurement decreases with an increasing number of detected photons (from 32% to 10% and 3.2% for Fig. 1.13(a–c), respectively). In turn, this leads to better reproducibility of the features over subsequent measurements.

Whereas in Fig. 1.13(a), it is quite impossible to tell whether there are two point sources or only one, Fig. 1.13(c) shows this clearly. Thus, whether it is possible to meet the Rayleigh criterion in practice depends strongly on the SNR of the measurement. Note that here, only intrinsic Poisson noise has been considered and that additional sources of noise will only further decrease the detectability and hence the attainable resolution.

Figure 1.13(b) shows a case intermediate between 1.13(a) and 1.13(c) in which two point sources are clearly suggested in the specimen, but the SNR of the measurements is insufficient to be absolutely certain. In such cases, *a priori* information about the specimen may help. Using the *a priori* information that the signal is the sum of exactly two distributions of known shape considerably increases the detectability of the position of the maxima of the individual intensity distributions. The resulting signal can then be fitted, in this case, to a sum of two identical responses (see Fig. 1.14). This permits accurately determining their relative position only by the noise in the signal, almost independent of the resolution of the system.

Having said all this, what can be expected of the resolution of a confocal fluorescence microscope? As discussed before, the confocal image results from (1) the excitation of the specimen from a point source and (2) the detection of the generated fluorescence through a conjugate point, the detection pinhole. Both the excitation and detection distribution are described by the PSF of the system. Under ideal circumstances and with the appropriate approximations, the PSF in the focal plane in the lateral direction is described by

$$I(v) \propto \left| \frac{2J_1(v)}{v} \right|^2, \tag{1.14}$$

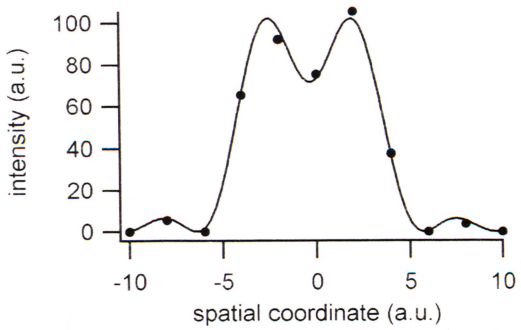

Figure 1.14 Fit of the data to the sum of two identical curves. The only free parameters in the fit are the positions of the maxima of the distributions and the amplitude of the distributions taken equal for each.

where the first minimum (zero) is found at $v_0 = 1.22\pi$; or, in real space units, using $v = r \cdot \mathrm{NA} \cdot 2\pi/\lambda$,

$$r_0 = \frac{0.61 \cdot \lambda}{\mathrm{NA}}. \tag{1.15}$$

Since the Rayleigh criterion states that two components of equal intensity should be considered to be just resolved when the principal intensity maximum of one coincides with the first intensity minimum of the other, r_0 is generally used to define the lateral resolution in a wide-field fluorescence microscope.

In a confocal fluorescence microscope, the generated fluorescence is imaged onto a detection pinhole. The resolution then is determined by the product of the excitation and detection PSF (see Sec. 1.2),

$$\mathrm{PSF}_{\mathrm{conf}} = \mathrm{PSF}_{\mathrm{exc}} \cdot \mathrm{PSF}_{\mathrm{det}}. \tag{1.16}$$

The excitation and detection PSF are equal in shape but slightly different in dimension because of the Stokes shift between excitation and detection ($\lambda_{\mathrm{exc}} < \lambda_{\mathrm{det}}$; see Sec. 2.4). Consider first the simplified case where $\lambda_{\mathrm{exc}} = \lambda_{\mathrm{det}}$. Then the confocal PSF is simply the square of the PSF of excitation,

$$\mathrm{PSF}_{\mathrm{conf}} = |\mathrm{PSF}_{\mathrm{exc}}|^2. \tag{1.17}$$

Clearly, in this case the Rayleigh criterion cannot be used directly to define the resolution in a confocal microscope since it is related to the position of the first minimum in the distribution. The position of this minimum does not change upon squaring the distribution. To circumvent this problem while retaining the convenience of the analytic expression of Eq. (1.15), one generally uses the FWHM of the distribution. As a reasonable approximation, the width of the lateral distribution (FWHM^r) equals the distance to the first minimum,

$$\mathrm{FWHM}^r \approx r_0. \tag{1.18}$$

1.3 What is the resolution?

The resolution of the microscope determines the smallest feature that can just be resolved, or the smallest distance that can be determined between features. Although vital for microscopy, resolution is not easily defined in general terms. The attainable resolution depends strongly on the signal-to-noise ratio (SNR) of the imaging system, on the imaging mode, and (sometimes strongly) on *a priori* knowledge of the specimen. An often-used resolution criterion is the Rayleigh criterion, which was first developed in connection with the resolving power of prism and grating spectroscopes. It states that two components of equal intensity should be considered to be just resolved when the principal intensity maximum of one coincides with the first intensity minimum of the other [Born and Wolf, 1980] (see Fig. 1.12). For this situation, an approximately 20% drop in intensity occurs between the two maxima (depending on the shape of the distributions).

But what is the effect of noise? In other words, what is the relation between the SNR of the measurement and the attainable resolution? The SNR is defined as

$$\mathrm{SNR} = \frac{|\text{mean signal} - \text{background}|}{\text{signal standard deviation}}. \tag{1.13}$$

All kinds of noise, e.g., shot, thermal, read-out, photon statistical, photon-scattering, and quantization, affect either the background level or the signal's standard deviation and will therefore decrease the SNR of the system. A decrease in SNR in turn decreases the visibility of the intensity decrease between the maxima as specified by the Rayleigh criterion. As an illustration, consider a fundamental property of any measurement of photons: Poisson noise. It can be shown [Goodman, 1985] that the measurement of a large number of uncorrelated and discrete events, such as the arrival of photons at a photodetector, will give rise to so-called Poisson statistics.

For instance, consider the detection of fluorescence emitted from a sample. The sample emits photons at a certain average rate, but the individual photons are ran-

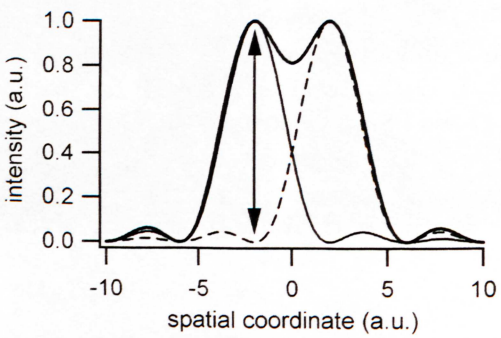

Figure 1.12 The Rayleigh criterion. Two components of equal intensity are resolved when the maximum of one coincides with the first minimum of the other. This results in an effective drop of the intensity between the two maxima of ~20%.

domly distributed over time. To determine the average fluorescence rate, the total number of photons emitted over a given time interval can be measured. Because of the random arrival of photons at the detector, repeating the measurement will yield a distribution of values. Hence, there remains an uncertainty in the true average value. For Poisson processes in particular, it means that if N photons are measured in a particular measurement, there is a 63% probability that the true average value is in the range between $N + \sqrt{N}$ and $N - \sqrt{N}$. For example, if N is 100 detected photons, a 63% probability exists that the true average value is in the range from 90 to 110. Because Poisson noise scales with $\sqrt{N}$, increasing the precision 10-fold, from $\pm 10\%$ to $\pm 1\%$, requires increasing the number of detected photons by a factor of 100, from 100 to 10,000. Poisson noise is an intrinsic property related to the detection of uncorrelated and discrete quantum events and cannot be avoided. Its relative importance can only be reduced by detecting as many photons as possible.

It is thus clear that whether the Rayleigh criterion is appropriate or not depends critically on the number of photons detected. To illustrate this point, consider the results of a numerical simulation shown in Fig. 1.13. The simulation involves the

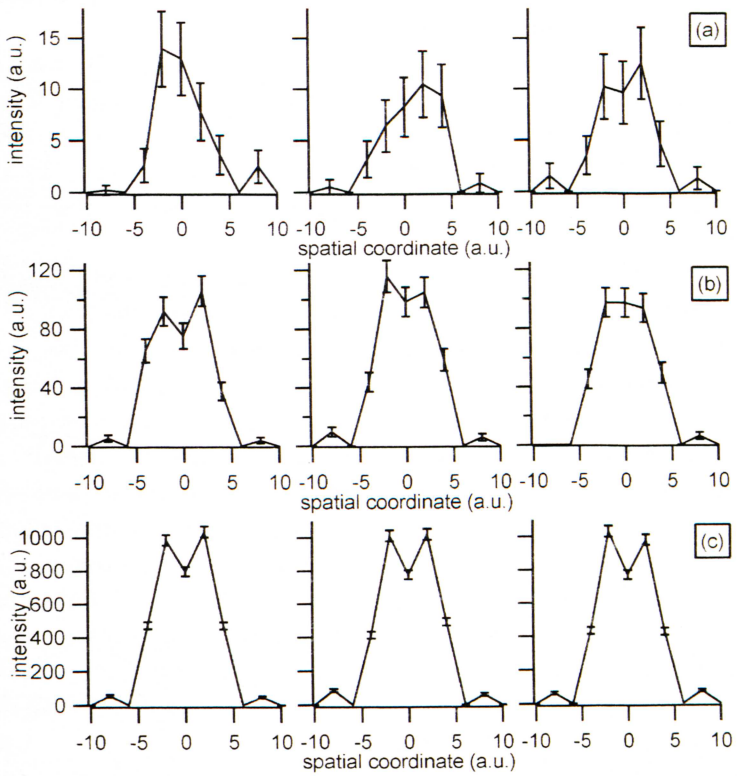

Figure 1.13 The influence of Poisson noise between two distributions, shifted spatially such that the maximum of the one coincides with the first minimum of the other (Rayleigh criterion). In this example, on average (a) 10, (b) 100, and (c) 1000 photons are detected from each intensity maximum. The reproducibility of each measurement is illustrated by the three subsequent measurements shown horizontally for each case.

measurement of photons emitted by two equally bright point sources that are separated by a distance exactly equal to the Rayleigh criterion. The signal is sampled along the spatial coordinate with a frequency that equals the Nyquist criterion. According to this criterion, a signal is sampled without artifacts only when it is sampled at a minimum of twice the frequency of the highest frequency present in the signal (see Chapter 4). In the case of the two point sources considered here, that corresponds to a sampling frequency of two samples per full-width-at-half-maximum (FWHM) of the signal distribution as a result of a single point source.

The difference between the simulated measurements shown in Figs. 1.13(a–c) is the maximum number of photons that are detected in each case. In Fig. 1.13(a) the maximum signal is on average 10 photons, whereas in Figs. 1.13(b) and 1.13(c) this number is 100 and 1000 photons respectively. It is assumed that only Poisson noise influences the measurement. Horizontally, three subsequent measurements are shown, where the changes are because of the random noise. The error bars denote the uncertainty in each measured value. The relative error of the measurement decreases with an increasing number of detected photons (from 32% to 10% and 3.2% for Fig. 1.13(a–c), respectively). In turn, this leads to better reproducibility of the features over subsequent measurements.

Whereas in Fig. 1.13(a), it is quite impossible to tell whether there are two point sources or only one, Fig. 1.13(c) shows this clearly. Thus, whether it is possible to meet the Rayleigh criterion in practice depends strongly on the SNR of the measurement. Note that here, only intrinsic Poisson noise has been considered and that additional sources of noise will only further decrease the detectability and hence the attainable resolution.

Figure 1.13(b) shows a case intermediate between 1.13(a) and 1.13(c) in which two point sources are clearly suggested in the specimen, but the SNR of the measurements is insufficient to be absolutely certain. In such cases, *a priori* information about the specimen may help. Using the *a priori* information that the signal is the sum of exactly two distributions of known shape considerably increases the detectability of the position of the maxima of the individual intensity distributions. The resulting signal can then be fitted, in this case, to a sum of two identical responses (see Fig. 1.14). This permits accurately determining their relative position only by the noise in the signal, almost independent of the resolution of the system.

Having said all this, what can be expected of the resolution of a confocal fluorescence microscope? As discussed before, the confocal image results from (1) the excitation of the specimen from a point source and (2) the detection of the generated fluorescence through a conjugate point, the detection pinhole. Both the excitation and detection distribution are described by the PSF of the system. Under ideal circumstances and with the appropriate approximations, the PSF in the focal plane in the lateral direction is described by

$$I(v) \propto \left| \frac{2J_1(v)}{v} \right|^2, \tag{1.14}$$

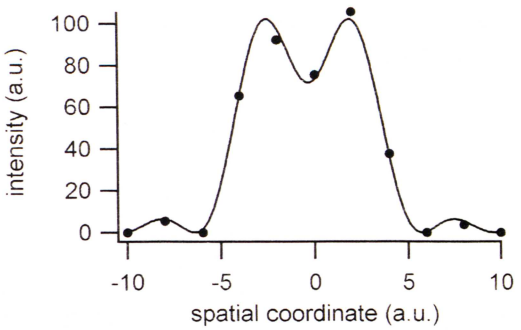

Figure 1.14 Fit of the data to the sum of two identical curves. The only free parameters in the fit are the positions of the maxima of the distributions and the amplitude of the distributions taken equal for each.

where the first minimum (zero) is found at $v_0 = 1.22\pi$; or, in real space units, using $v = r \cdot \mathrm{NA} \cdot 2\pi/\lambda$,

$$r_0 = \frac{0.61 \cdot \lambda}{\mathrm{NA}}. \tag{1.15}$$

Since the Rayleigh criterion states that two components of equal intensity should be considered to be just resolved when the principal intensity maximum of one coincides with the first intensity minimum of the other, r_0 is generally used to define the lateral resolution in a wide-field fluorescence microscope.

In a confocal fluorescence microscope, the generated fluorescence is imaged onto a detection pinhole. The resolution then is determined by the product of the excitation and detection PSF (see Sec. 1.2),

$$\mathrm{PSF}_{\mathrm{conf}} = \mathrm{PSF}_{\mathrm{exc}} \cdot \mathrm{PSF}_{\mathrm{det}}. \tag{1.16}$$

The excitation and detection PSF are equal in shape but slightly different in dimension because of the Stokes shift between excitation and detection ($\lambda_{\mathrm{exc}} < \lambda_{\mathrm{det}}$; see Sec. 2.4). Consider first the simplified case where $\lambda_{\mathrm{exc}} = \lambda_{\mathrm{det}}$. Then the confocal PSF is simply the square of the PSF of excitation,

$$\mathrm{PSF}_{\mathrm{conf}} = |\mathrm{PSF}_{\mathrm{exc}}|^2. \tag{1.17}$$

Clearly, in this case the Rayleigh criterion cannot be used directly to define the resolution in a confocal microscope since it is related to the position of the first minimum in the distribution. The position of this minimum does not change upon squaring the distribution. To circumvent this problem while retaining the convenience of the analytic expression of Eq. (1.15), one generally uses the FWHM of the distribution. As a reasonable approximation, the width of the lateral distribution (FWHM^r) equals the distance to the first minimum,

$$\mathrm{FWHM}^r \approx r_0. \tag{1.18}$$

The FWHM of the lateral confocal PSF ($\mathrm{FWHM}^r_{\mathrm{conf}}$) is then determined by the square of the excitation PSF and hence

$$\begin{aligned}\mathrm{FWHM}^r_{\mathrm{conf}} &\approx \frac{1}{\sqrt{2}}\mathrm{FWHM}^r_{\mathrm{exc}} \\ &\approx \frac{0.61 \cdot \lambda_{\mathrm{exc}}}{\sqrt{2} \cdot \mathrm{NA}}.\end{aligned} \tag{1.19}$$

The factor of $1/\sqrt{2}$ appearing in Eq. (1.19) can be easily derived when assuming a Gaussian-shaped PSF. However, inspection shows that it is true also to an excellent approximation for the PSF distributions described here. Because the wavelength of detection is always longer than that of the excitation, the effective lateral resolution for the confocal microscope is lower than specified in Eq. (1.19). Taking the ratio of the excitation and detection wavelength as $\beta = \lambda_{\mathrm{exc}}/\lambda_{\mathrm{det}}$, it can be shown (again, assuming Gaussian-shaped PSFs) that the FWHM of the confocal distribution (i.e., a measure of the lateral resolution in a confocal microscope) is approximately given by

$$\begin{aligned}\mathrm{FWHM}^r_{\mathrm{conf}} &\approx \frac{1}{\sqrt{1+\beta^2}} \cdot \mathrm{FWHM}^r_{\mathrm{exc}} \\ &\approx \frac{1}{\sqrt{1+\beta^2}} \cdot \frac{0.61 \cdot \lambda_{\mathrm{exc}}}{\mathrm{NA}}.\end{aligned} \tag{1.20}$$

Note that in this derivation, an infinitely small detection pinhole is assumed. The influence of the pinhole size on the resolution is discussed in Sec. 2.3.

Using similar arguments, the axial resolution of a confocal fluorescence microscope can be defined. The PSF of the system in the axial direction is

$$I(u) \propto \left(\frac{\sin(u/4)}{u/4}\right)^2, \tag{1.21}$$

where the first zero is at $u_0 = 4\pi$. Or, in real space units, using $u = z \cdot (\mathrm{NA}^2/n) \cdot 2\pi/\lambda$, where z is the axial position relative to the geometrical focal point,

$$z_0 = \frac{2 \cdot n \cdot \lambda}{(\mathrm{NA})^2}. \tag{1.22}$$

In terms of the Rayleigh criterion, u_0 defines the axial resolution in a wide-field fluorescence microscope. Note that this definition of axial resolution for a wide-field microscope is not generally applicable. It applies well to, for instance, two axially separated small fluorescing beads. It cannot, however, directly be generalized to other cases. For instance, in a wide-field microscope, the fluorescence generated by a thin fluorescing layer is equal for each axial plane. Hence it is impossible to

determine focus for such an object or to resolve an axial separation between two such layers. Equation (1.22) should thus be used with care when used to describe axial resolution. In fact, the Rayleigh criterion is useful only for one-dimensional problems. It becomes ambiguous when applied to objects having a 2D or a 3D structure. Just as it does not apply to the axial separation of thin layers, it also does not apply to the lateral separation of two axially elongated cylinders, for example.

In a confocal fluorescence microscope, the situation is less ambiguous. Here, the detection pinhole suppresses fluorescence from out-of-focus planes, providing true axial resolution. Again, the first minimum in the axial distribution needs to be related to the width of the PSF (FWHM^z) to permit a definition of the confocal axial resolution as

$$\mathrm{FWHM}^z \approx z_0. \tag{1.23}$$

Assuming equal wavelength of excitation and detection ($\lambda_{\mathrm{exc}} = \lambda_{\mathrm{det}}$), the axial confocal PSF is again proportional to the square of the excitation PSF, with a FWHM ($\mathrm{FWHM}^z_{\mathrm{conf}}$) given by

$$\begin{aligned} \mathrm{FWHM}^z_{\mathrm{conf}} &\approx \frac{1}{\sqrt{2}} \cdot \mathrm{FWHM}^z_{\mathrm{exc}} \\ &\approx \frac{1}{\sqrt{2}} \cdot \frac{2 \cdot n \cdot \lambda_{\mathrm{exc}}}{(\mathrm{NA})^2}. \end{aligned} \tag{1.24}$$

Taking the difference in wavelength between excitation and detection into account, the axial resolution in a confocal microscope is defined by

$$\mathrm{FWHM}^z_{\mathrm{conf}} \approx \frac{1}{\sqrt{1+\beta^2}} \cdot \frac{2 \cdot n \cdot \lambda_{\mathrm{exc}}}{(\mathrm{NA})^2}. \tag{1.25}$$

All formulas given here are approximate in some sense. For instance, the basic formulae describing the lateral and axial PSF [Eqs. (1.14) and (1.21)] result from a number of approximations to derive analytical solutions to the full diffraction theory that describes the focal field of a high-NA lens. Further approximations are made to relate the minima in the distributions to the FWHM and to take the difference in wavelength between excitation and detection into account. Appendix B summarizes the relations described here and compares them to the results of numerical calculations based on scalar diffraction theory. Nevertheless, these basic formulae provide good practical approximations to the lateral and axial resolution in a confocal fluorescence microscope.

To give a feeling for practical numbers, some typical values for general dyes used in confocal fluorescence microscopy are given in Table 1.1. For the highest possible resolution, both excitation and detection wavelengths should be as short as possible. However, some practical considerations limit the choice in wavelengths. First, short-wavelength excitation (i.e., blue or near UV) is generally biologically

Table 1.1a Maximum excitation and detection wavelengths and generally available excitation laser wavelengths for common dyes.

Dye	λ_{exc} (nm)	λ_{det} (nm)	λ_{laser} (nm)
DAPI	350	470	351
FITC	490	520	488
Rhodamine 6G	530	556	488
Texas Red	595	615	543
Alexa 594	590	617	543
Cy5	649	670	633

Table 1.1b Attainable resolution in confocal fluorescence microscopy [Eqs. (1.17) and (1.22)] for common dyes (using NA = 1.3 and $n = 1.518$).

Dye	β	$FWHM^r_{conf}$ (nm)	$FWHM^z_{conf}$ (nm)
DAPI	0.75	132	505
FITC	0.94	167	639
Rhodamine 6G	0.88	172	659
Texas Red	0.88	191	731
Alexa 594	0.88	191	732
Cy5	0.94	216	827

much more damaging than longer-wavelength excitation. Also, chromatic aberrations generally increase strongly towards the UV. Furthermore, only a limited number of excitation wavelengths are available, determined by the laser(s) installed in the microscope. For a given wavelength of excitation, the Stokes shift should be kept at a minimum (i.e., β close to one) to provide the maximum benefit of confocal detection. The difference between excitation and detection should, however, be large enough to permit scattered photons at the excitation wavelength to be blocked from reaching the detector. As a general rule, an efficient blocking filter requires the detection wavelength to be Stokes shifted by at least 7% of the excitation wavelength. Hence, for an excitation wavelength of $\lambda_{exc} = 488$ nm, a suitable blocking filter can be designed only for detection wavelengths of $\lambda_{det} \geq 522$ nm.

Note that the axial resolution is worse by a factor of $3.3/\sin\alpha$ (i.e., $\approx$3.9 for NA = 1.3) than the lateral resolution. This factor depends only on the semi-aperture angle (α) and increases strongly for decreasing NA.

1.3.1 Resolution and the OTF

So far, resolution has been discussed in the spatial domain, i.e., in relation to the PSF. Alternatively, the optical performance of a microscope can be specified in terms of the OTF. The OTF shows to what extent various spatial frequencies are transmitted by the optical system. Because of the limited NA of a microscope, a sharp cut-off frequency occurs beyond where spatial frequencies are transmitted. For a wide-field fluorescence microscope, the lateral and axial cut-off frequencies are $\Omega_{lat} = 2 \cdot NA/\lambda$ and $\Omega_{ax} = n \cdot (1 - \cos\alpha)/\lambda$ respectively.

How does this relate to the previously defined resolution criteria in the spatial domain of $r_0 = 0.61 \cdot \lambda/\mathrm{NA}$ and $z_0 = 2 \cdot n \cdot \lambda/(\mathrm{NA})^2$?

The first node in the lateral PSF corresponds to a spatial frequency of

$$\Omega_{r_0} = \frac{1.64 \cdot \mathrm{NA}}{\lambda}. \tag{1.26a}$$

Thus, for a microscope objective with a NA = 1.3, the first lateral node corresponds to a spatial frequency of $\Omega_{r_0} \approx 2.1\lambda^{-1}$. The lateral cut-off frequency (Ω_{lat}) at this NA is $2.6\lambda^{-1}$. The lateral resolution criterion therefore corresponds to a spatial frequency slightly lower than the cut-off frequency. The difference between the two figures is because of the fact that they result from different definitions. Similarly, for the axial direction, the spatial frequency corresponding to the axial resolution criterion is

$$\Omega_{z_0} = \frac{(\mathrm{NA})^2}{2n\lambda}, \tag{1.26b}$$

which is slightly less than the axial cut-off frequency of $\Omega_{\mathrm{ax}} = n(1 - \cos\alpha)/\lambda$. Again, the difference between the two values results from the use of different definitions.

It was found in the previous section that the lateral and axial cut-off frequencies in a confocal fluorescence microscope are twice those of a wide-field microscope. Potentially, the resolution of a confocal microscope is thus twice that of a wide-field microscope. Note that the Rayleigh criterion predicts an improvement of the resolution of a factor of only $\sqrt{2}$. The difference again is due to the different ways in which the resolution is defined. Note also that, just as in the case of a resolution criterion in terms of the spatial coordinates, a resolution criterion in terms of the OTF should consider the influence of the SNR. In other words, what it is the minimum detectable amplitude of a particular spatial frequency? Only frequencies above this limit will be detected and hence will determine the attainable resolution in practice.

1.3.2 Magnification

Finally, what is the relation between resolution and magnification? Figure 1.15 illustrates this issue. The images on the right side are magnified copies of a part of the images on the left side. The magnification factor is 4.3. The top-row images have been created at high resolution (600 pixels/inch), whereas the resolution of the bottom-row images is six times lower (100 pixels/inch). Clearly, magnification enlarges the image but does not provide more detail. It only helps to visualize the detail present in the original image. Thus, magnification and resolution are independent. Increasing the magnification does *not* increase the resolution. Only if the resolution is sufficient can magnification facilitate in visualizing small features.

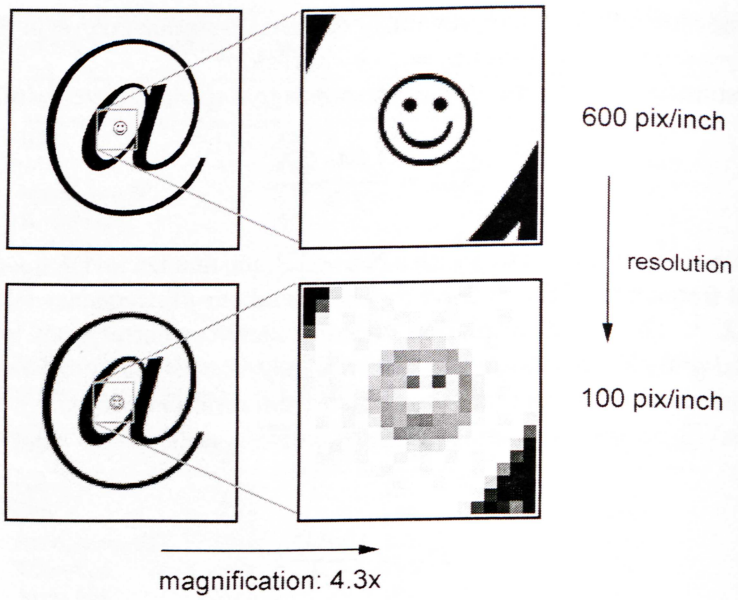

Figure 1.15 Magnification and resolution are independent quantities.

1.4 Optical aberrations

Optical aberrations, both in the excitation and the detection paths of the confocal fluorescence microscope, degrade its imaging performance. In the absence of aberrations, the microscope provides maximum resolution, limited only by diffraction. Every aberration will distort the wave propagation through the system and cause a loss in resolution compared to this diffraction-limited optimum. In a confocal fluorescence microscope, a loss in resolution is generally accompanied by a decrease in signal strength and sensitivity. Aberrations in the excitation path lead to a spreading of the excitation PSF, thereby distributing the excitation light over a larger volume. In turn, aberrations in the detection path give rise to a spreading of the detection PSF. Fluorescence emitted from a single point is imaged onto the detection pinhole to a spot larger than expected from diffraction alone, reducing the amount of light passing through the pinhole. This loss in detected fluorescence can only be avoided by enlarging the pinhole, thereby compromising the resolution.

The optical design of commercial confocal fluorescence microscopes minimizes optical aberrations (see Sec. A.2). Generally, however, two causes of aberration are present: chromatic aberrations and aberrations induced by a refractive index mismatch.

1.4.1 Chromatic aberration

A lens or imaging system that has chromatic aberration possesses imaging properties that vary with wavelength. Generally, this appears to be a dependence of

the focal length (chromatic focal shift) and lateral magnification (lateral color) on the wavelength. In confocal fluorescence microscopy, chromatic aberrations influence the imaging properties in two ways, causing: (1) shifts (both laterally, for off-axis operation, and axially) in the excitation PSF, since different excitation wavelengths focus at different positions; and (2) lateral and axial shifts in the detection PSF, since different emission wavelengths will be imaged at different positions, e.g., when multiple labeled specimens are used. The degree to which chromatic aberrations influence the imaging properties strongly depends on the microscope objective and the range of wavelengths used in excitation and detection. Microscope objectives are generally corrected for either two (achromats) or three (apochromats) wavelengths (see Sec. 2.1). This means that for these particular wavelengths, the aberrations are optimally balanced and minimized. Between these wavelengths, the microscope objective generally still performs well, but outside this wavelength region the aberrations usually grow exponentially, particularly towards the shorter wavelengths. Especially in the UV, chromatic aberrations can become severe. There is no rule or estimate for the magnitude of the chromatic aberrations. They must be determined for each microscope and microscope objective.

Calibration becomes especially important when comparing positions of species labeled with different fluorophores. For this purpose, multiple labeled fluorescing beads are commercially available. (Note that lateral shifts between images of different fluorescence or absorption wavelength of multiple labeled specimens may also result from misalignment of the filters and dichroics within the microscope.)

The simultaneous use of a number of different fluorophores requires special care in confocal fluorescence microscopy, even in the absence of chromatic aberration. The lateral and axial size of the PSF, both in excitation and emission, depends linearly on the wavelength. Hence, the size of the detection pinhole (see Sec. 2.3) needs to be optimized for each detection wavelength in order to obtain comparable image conditions for each fluorophore.

1.4.2 Refractive index mismatch

Microscope objectives are designed to operate under specific optical conditions. For instance, an oil-immersion objective is designed to provide optimal imaging conditions when used with an immersion oil with the specified refractive index, a cover glass of the correct thickness and of specific material, and a specimen embedded in a medium with the same refractive index as the immersion oil. However, in practice, high-NA oil-immersion microscope objectives are often used for microscopy on biological samples, which generally consist primarily of water. In this case, a refractive index mismatch exists between the microscope objective and the specimen medium. This mismatch deteriorates the imaging properties of the system.

What causes the aberrations induced by the refractive index mismatch? The problem is schematically depicted in Fig. 1.16. Figure 1.16(a) shows the ideal situation, in which the immersion medium, cover glass, and mounting medium all have

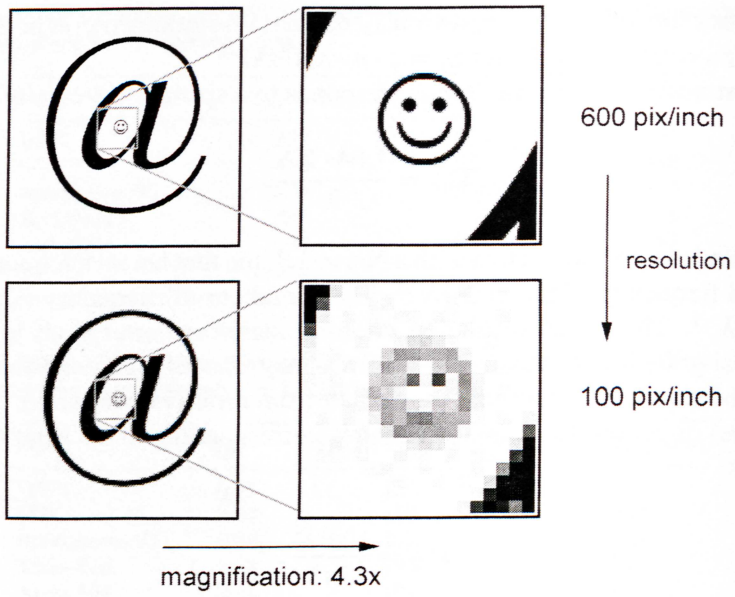

Figure 1.15 Magnification and resolution are independent quantities.

1.4 Optical aberrations

Optical aberrations, both in the excitation and the detection paths of the confocal fluorescence microscope, degrade its imaging performance. In the absence of aberrations, the microscope provides maximum resolution, limited only by diffraction. Every aberration will distort the wave propagation through the system and cause a loss in resolution compared to this diffraction-limited optimum. In a confocal fluorescence microscope, a loss in resolution is generally accompanied by a decrease in signal strength and sensitivity. Aberrations in the excitation path lead to a spreading of the excitation PSF, thereby distributing the excitation light over a larger volume. In turn, aberrations in the detection path give rise to a spreading of the detection PSF. Fluorescence emitted from a single point is imaged onto the detection pinhole to a spot larger than expected from diffraction alone, reducing the amount of light passing through the pinhole. This loss in detected fluorescence can only be avoided by enlarging the pinhole, thereby compromising the resolution.

The optical design of commercial confocal fluorescence microscopes minimizes optical aberrations (see Sec. A.2). Generally, however, two causes of aberration are present: chromatic aberrations and aberrations induced by a refractive index mismatch.

1.4.1 Chromatic aberration

A lens or imaging system that has chromatic aberration possesses imaging properties that vary with wavelength. Generally, this appears to be a dependence of

the focal length (chromatic focal shift) and lateral magnification (lateral color) on the wavelength. In confocal fluorescence microscopy, chromatic aberrations influence the imaging properties in two ways, causing: (1) shifts (both laterally, for off-axis operation, and axially) in the excitation PSF, since different excitation wavelengths focus at different positions; and (2) lateral and axial shifts in the detection PSF, since different emission wavelengths will be imaged at different positions, e.g., when multiple labeled specimens are used. The degree to which chromatic aberrations influence the imaging properties strongly depends on the microscope objective and the range of wavelengths used in excitation and detection. Microscope objectives are generally corrected for either two (achromats) or three (apochromats) wavelengths (see Sec. 2.1). This means that for these particular wavelengths, the aberrations are optimally balanced and minimized. Between these wavelengths, the microscope objective generally still performs well, but outside this wavelength region the aberrations usually grow exponentially, particularly towards the shorter wavelengths. Especially in the UV, chromatic aberrations can become severe. There is no rule or estimate for the magnitude of the chromatic aberrations. They must be determined for each microscope and microscope objective.

Calibration becomes especially important when comparing positions of species labeled with different fluorophores. For this purpose, multiple labeled fluorescing beads are commercially available. (Note that lateral shifts between images of different fluorescence or absorption wavelength of multiple labeled specimens may also result from misalignment of the filters and dichroics within the microscope.)

The simultaneous use of a number of different fluorophores requires special care in confocal fluorescence microscopy, even in the absence of chromatic aberration. The lateral and axial size of the PSF, both in excitation and emission, depends linearly on the wavelength. Hence, the size of the detection pinhole (see Sec. 2.3) needs to be optimized for each detection wavelength in order to obtain comparable image conditions for each fluorophore.

1.4.2 Refractive index mismatch

Microscope objectives are designed to operate under specific optical conditions. For instance, an oil-immersion objective is designed to provide optimal imaging conditions when used with an immersion oil with the specified refractive index, a cover glass of the correct thickness and of specific material, and a specimen embedded in a medium with the same refractive index as the immersion oil. However, in practice, high-NA oil-immersion microscope objectives are often used for microscopy on biological samples, which generally consist primarily of water. In this case, a refractive index mismatch exists between the microscope objective and the specimen medium. This mismatch deteriorates the imaging properties of the system.

What causes the aberrations induced by the refractive index mismatch? The problem is schematically depicted in Fig. 1.16. Figure 1.16(a) shows the ideal situation, in which the immersion medium, cover glass, and mounting medium all have